

Supplementary Data

Structural insights into CpG-specific DNA methylation by human DNA methyltransferase DNMT3B

Chien-Chu Lin¹, Yi-Ping Chen¹, Wei-Zen Yang¹, James C. K. Shen¹ and
Hanna S. Yuan^{1,2*}

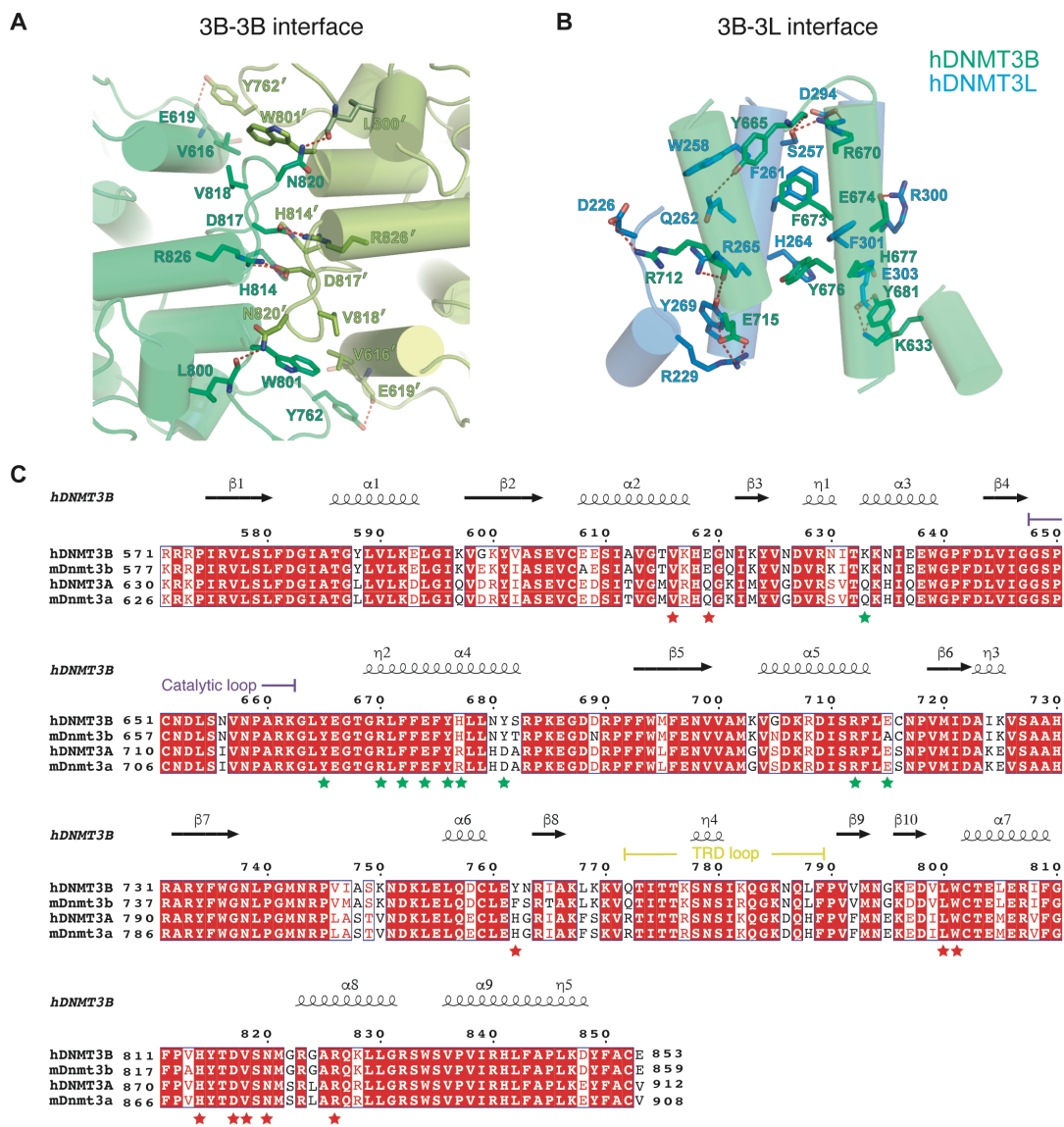
¹Institute of Molecular Biology, Academia Sinica, Taipei, Taiwan 11529, ROC.

²Graduate Institute of Biochemistry and Molecular Biology, National Taiwan University,
Taipei, Taiwan 10048, ROC.

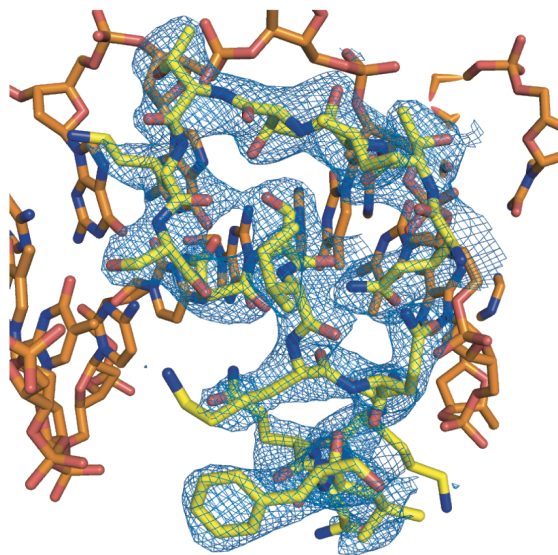
This file contains:
Supplementary Table S1
Supplementary Figures S1-6

Supplementary Table S1.
Oligonucleotides and DNA substrates used in crystallization and activity assays.

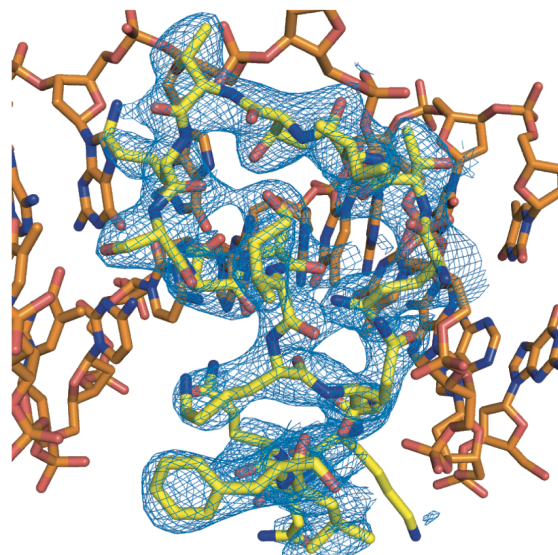
Experiment	Name	Sequence (5'-to-3')
Crystallization	CpGpG	GAATT CGG AAAAATTTTTCCGAATT
	CpGpT	GCATG CGT TCTAATTAGAACGCATG
MTase-Glo assay	CG	AATT CG AAAAAATTTTTTCGAATT
	CA	AATT CA AAAAAATTTTTTTGAATT
	CT	AATT CT AAAAAATTTTTTAGAATT
	CGG	AATT CGG AAAAAATTTTTCCGAATT
	CGA	AATT CGA AAAAAATTTTTTCGAATT
	CGT	AATT CGT AAAAAATTTTTACGAATT
	CG-2	Forward: AAAA CG AAAAAAAAAAAAAAAAAAAA Reverse: TTTTTTTTTTTTTTTTTTCGTTTT
	CG-3	Forward: AAAA CG AAAAAAAAAAAAAAAAAAAAAAAAAAAA AAAAAAAAAAAAAAAAAAAA Reverse: TTTTTTTTTTTTTTTTTTTTTTTTTTTTTTTTTTTT TTTTT CG TTTT
Methylation-coupled restriction enzyme cleavage assay	494-bp DNA substrate	GGCCGTTCTTCTGGATGTTTGAGAATGTTGTAGCC ATGAAGGTTGGCGACAAGAGGGACATCTCACGG TTCCTGGAGTGTAATCCAGTGATGATTGATGCCA TCAAAGTTTCTGCTGCTCACAGGGCCCGATACTT CTGGGGCAACCTAC CCGG GATGAACAGGCCCGTG ATAGCATCAAAGAATGATAAACTCGAGCTGCAG GACTGCTTGGAAACAATAGGATAGCCAAGTTAA AGAAAGTACAGACAATAACCACCAAGTCGA CGATCAAACAGGGGAAAAACCAACTTTCCCTGT TGTCATGAATGGCAAAGAAGATGTTTTGTGGTGC ACTGAGCTCGAAAGGATCTTTGGCTTTCCTGTGC ACTACACAGACGTGTCCAACATGGGCCGTGGTGC CCGCCAGAAGCTGCTGGGAAGGTCTGGAGCGTG CCTGTCATCCGACACCTCTTCGCCCTCTGAAGG ACTACTTTGCATGTGAATAG
Fluorescence polarization assay	3'-FAM-labeled CG-3	Forward: AAAA CG AAAAAAAAAAAAAAAAAAAAAAAAAAAA AAAAAAAAAAAAAAAAAAAA-FAM Reverse: TTTTTTTTTTTTTTTTTTTTTTTTTTTTTTTTTTTT TTTTT CG TTTT



Supplementary Figure S1. Conserved residues are located in the DNMT3B-3L interfaces. (A-B) Amino acids located in the 3B-3B and 3B-3L interfaces are shown by the stick models, in green for those of DNMT3B and in blue for those of DNMT3L. **(C)** Sequence alignment of the methyltransferase catalytic domain of human hDNMT3B, mouse mDnmt3b, human hDNMT3A and mouse mDnmt3a. Secondary structures of DNMT3B derived from the crystal structure of the DNMT3B-3L-DNA (CpGpG) complex (PDB entry: 6KDA) are shown above the sequences. The conserved residues located in the 3B-3B and 3B-3L interfaces are marked with green and red stars below the sequences, respectively.

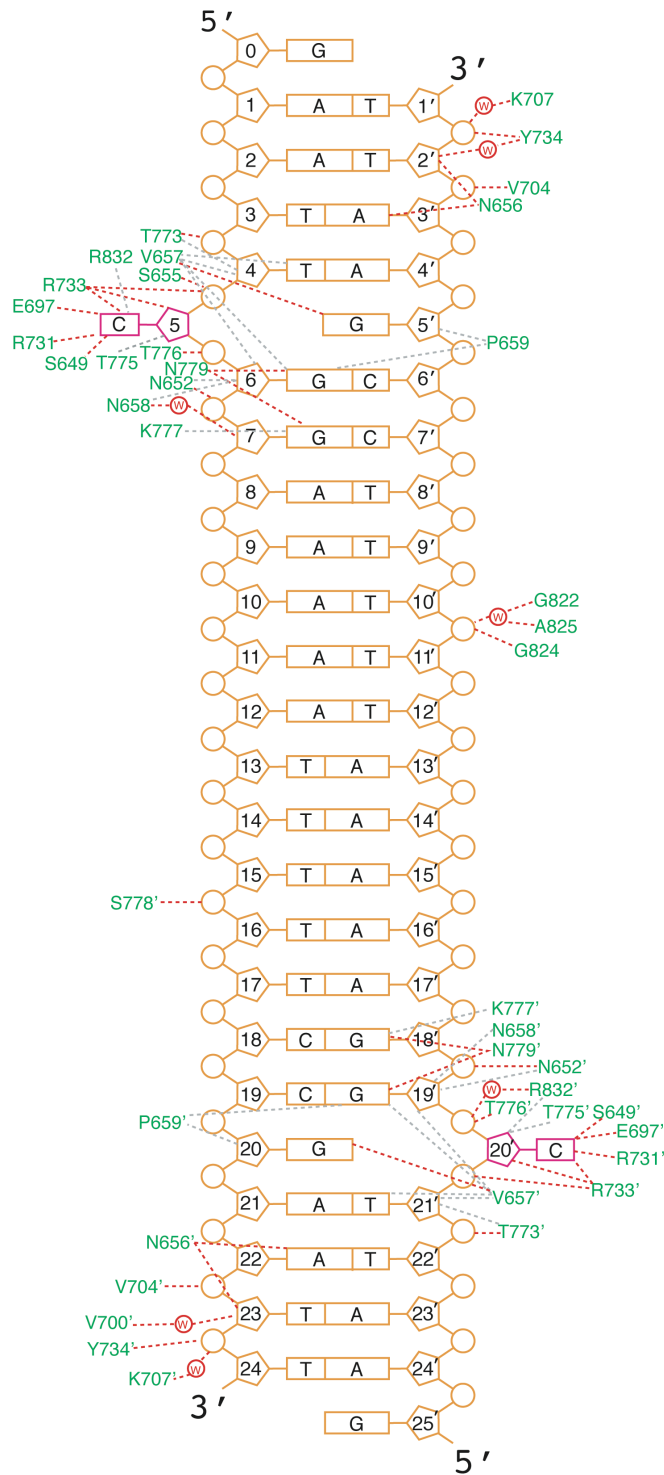


TRD loop of 3B protomer

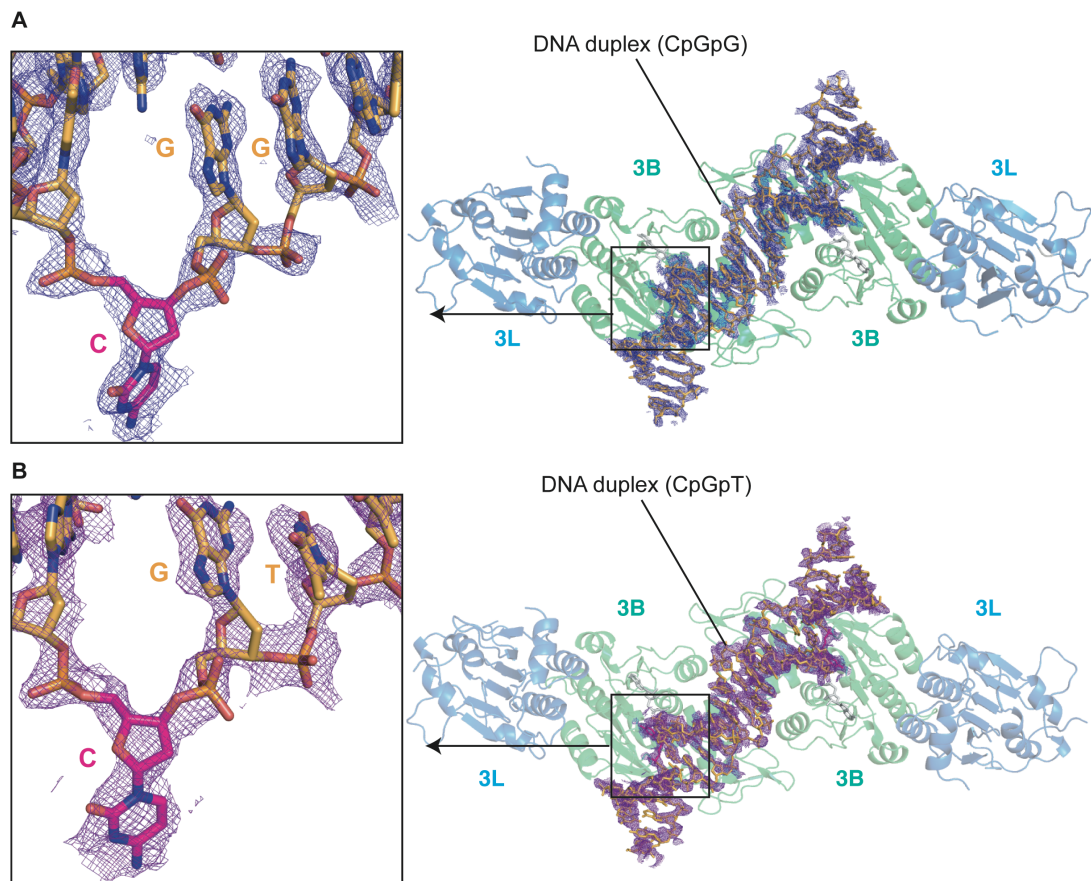


TRD loop of 3B' protomer

Supplementary Figure S2. TRD loops of DNMT3B interacts at the major groove of DNA duplex in the crystal structure of DNMT3B-3L-DNA (CpGpG). The electron density maps (2Fo-Fc) of TRD loops are contoured at 1σ level. The average B-factor of TRD loops is 53.03 \AA^2

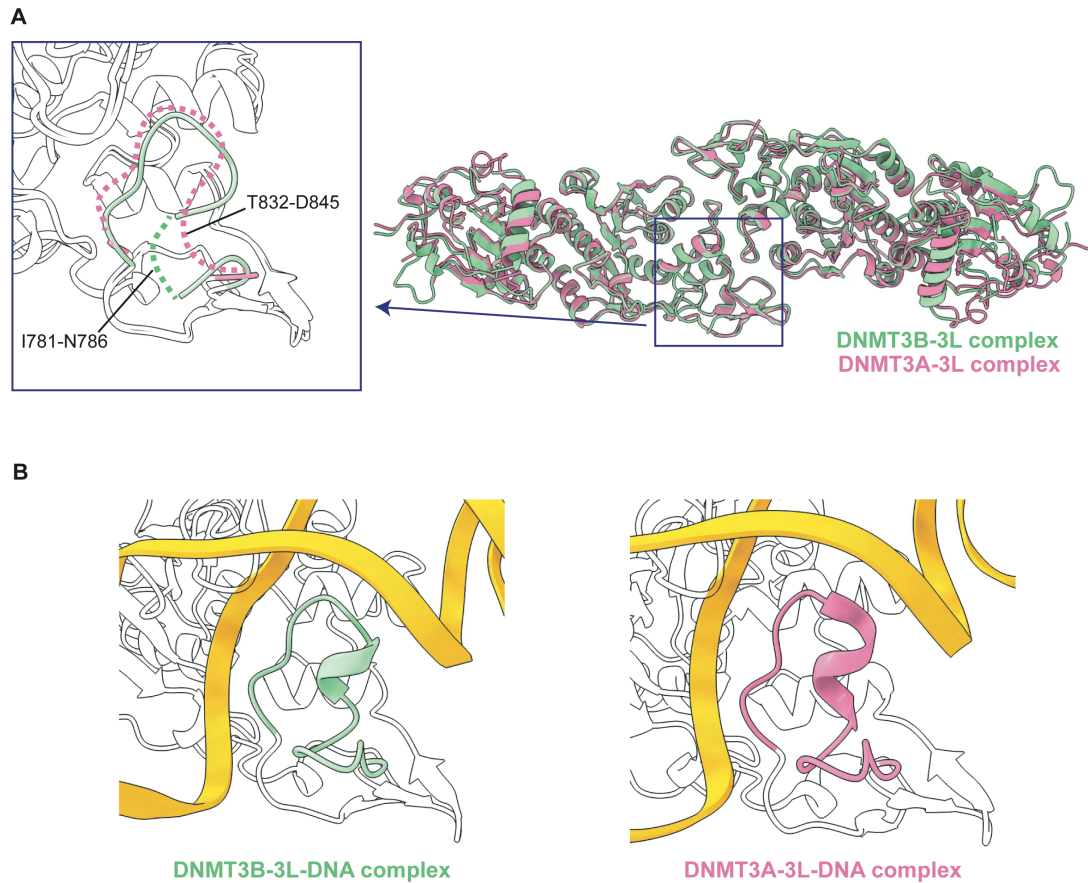


Supplementary Figure S3. Schematic diagram of the interactions between DNMT3B and DNA. The hydrogen bonds and van der Waals contacts are shown as red and gray dashed lines, respectively. Water molecules are shown as the letter “w” enclosed in a red circle.

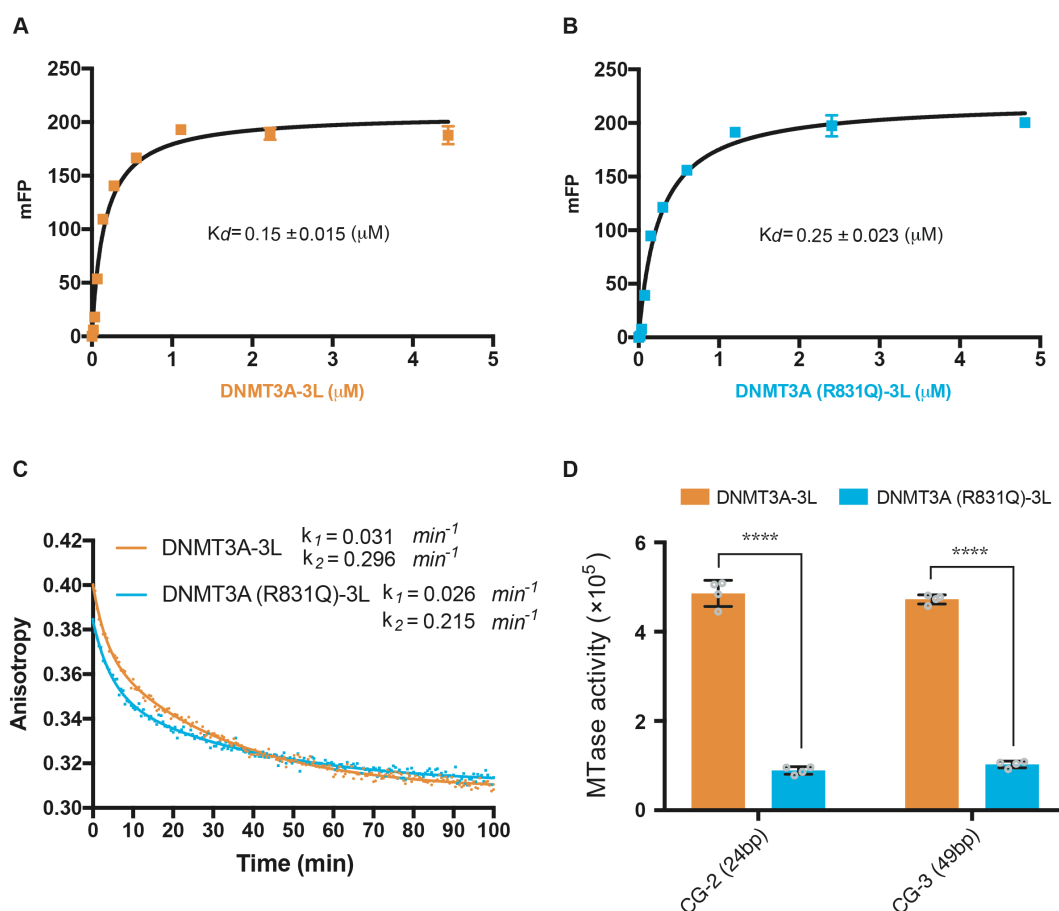


Supplementary Figure S4. Electron density for the DNA in the crystal structures of DNMT3B-3L-DNA (CpGpG) and DNMT3B-3L-DNA (CpGpT) complexes.

(A-B) The DNA duplexes (CpGpG) and (CpGpT) are shown as orange stick models. Cytosines of CpGpG and CpGpT sites are colored magenta. Zoomed-in views (left) of the CpGpG and CpGpT sites are shown with a feature-enhanced map contoured at 1.8 σ level.



Supplementary Figure S5. The stable TRD loop contributes to the processivity of DNMT3B. (A) Superimposition of the DNA-free form of the catalytic domains of DNMT3A (pink) and DNMT3B (green) reveals that the TRD loop is completely disordered in DNMT3A but less flexible in DNMT3B (only six residues 781-786 are disordered). (B) Cartoon representations of TRD loops of DNMT3B (green, the left panel) and DNMT3A (pink, the right panel) bound with DNA duplex (orange).



Supplementary Figure S6. DNA binding and methylation activity of human DNMT3A-3L and DNMT3A (R831Q)-3L. (A-B) Dissociation constants (K_d) of DNMT3A-3L and DNMT3A (R831Q)-3L complexes upon binding with the 49-bp FAM-labeled DNA (CG-3) were measured by fluorescence polarization ($n=3$). R831 in DNMT3A directly involved in DNA interactions and thus the R831Q mutant had a decreased DNA binding activity. (C) Dissociation rate constants (k_1 and k_2) for DNMT3A-3L and DNMT3A (R831Q)-3L complexes were determined by measuring the decreasing signal of fluorescence anisotropy of FAM-labeled GC-3 using unlabeled DNA as competitors. (D) Methylation activities of DNMT3A-3L and DNMT3A (R831Q)-3L for DNA of different lengths were measured by methyltransferase-Glo assays (in Luminescence, RLU, $n=4$; error bars denote SD; **** represents $P<0.0001$). Statistical significance (P values) was determined by two-tailed Student's t -test.